






ORIGINAL RESEARCH

# Validating a Curvature-Based Marker of Cervical Carotid Tortuosity for Risk Assessment in Heritable Aortopathies

Jin Vivian Lee , MD, MS; Anna L. Huguenard , MD; Ralph G. Dacey , MD; Alan C. Braverman , MD; Joshua W. Osburn , MD

**BACKGROUND:** Cervical arterial tortuosity is associated with adverse outcomes in Loeys-Dietz syndrome and other heritable aortopathies.

**METHODS AND RESULTS:** A method to assess tortuosity based on curvature of the vessel centerline in 3-dimensional space was developed. We measured cervical carotid tortuosity in 65 patients with Loeys-Dietz syndrome from baseline computed tomography angiogram/magnetic resonance angiogram and all serial images during follow-up. Relations between baseline carotid tortuosity, age, aortic root diameter, and its change over time were compared. Patients with unoperated aortic roots were assessed for clinical end point (type A aortic dissection or aortic root surgery during 4 years of follow-up). Logistic regression was performed to assess the likelihood of clinical end point according to baseline carotid tortuosity. Total absolute curvature at baseline was  $11.13 \pm 5.76$  and was relatively unchanged at 8 to 10 years (fold change:  $0.026 \pm 0.298$ ,  $P=1.00$ ), whereas tortuosity index at baseline was  $0.262 \pm 0.131$ , with greater variability at 8 to 10 years (fold change:  $0.302 \pm 0.656$ ,  $P=0.818$ ). Baseline total absolute curvature correlated with aortic root diameter ( $r=0.456$ ,  $P=0.004$ ) and was independently associated with aortic events during the 4-year follow-up (adjusted odds ratio [OR], 2.64 [95% CI, 1.02–6.85]). Baseline tortuosity index correlated with age ( $r=0.532$ ,  $P<0.001$ ) and was not associated with events (adjusted OR, 1.88 [95% CI, 0.79–4.51]). Finally, baseline total absolute curvature had good discrimination of 4-year outcomes (area under the curve= $0.724$ ,  $P=0.014$ ), which may be prognostic or predictive.

**CONCLUSIONS:** Here we introduce cervical carotid tortuosity as a promising quantitative biomarker with validated, standardized characteristics. Specifically, we recommend the adoption of a curvature-based measure, total absolute curvature, for early detection or monitoring of disease progression in Loeys-Dietz syndrome.

**Key Words:** aortic dissection ■ arterial tortuosity ■ genetics ■ LDS ■ thoracic aortic aneurysm

Arterial tortuosity and aneurysms are distinctive features in heritable aortopathies like Loeys-Dietz syndrome (LDS) and Marfan syndrome.<sup>1</sup> Aortic size, routinely monitored in clinical practice, is one of the strongest predictors of ascending (type A) aortic dissection risk in both LDS and Marfan syndrome. However, a notable distinction exists; the associated risks of aortic dissection and rupture manifest

at a younger age and smaller aortic diameters in LDS than in Marfan syndrome.<sup>2–4</sup> This divergence sets LDS clinically apart, often leading to a more aggressive vascular disease. Consequently, consideration for prophylactic aortic root surgery in LDS occurs earlier, potentially at diameters above 40 to 45 mm, reflecting the heightened risk associated with this connective tissue disorder.<sup>5–7</sup>

Correspondence to: Joshua W. Osburn, MD, FAANS, FACS, FAHA, Department of Neurological Surgery, Washington University School of Medicine, 660 S. Euclid Avenue, Campus Box 8057, St. Louis, MO 63110. Email: [josbun@wustl.edu](mailto:josbun@wustl.edu)

This article was sent to Erik B. Schelbert, MD, MS, Associate Editor, for review by expert referees, editorial decision, and final disposition.

Supplemental Material is available at <https://www.ahajournals.org/doi/suppl/10.1161/JAHA.124.035171>

For Sources of Funding and Disclosures, see page 12.

© 2024 The Author(s). Published on behalf of the American Heart Association, Inc., by Wiley. This is an open access article under the terms of the [Creative Commons Attribution-NonCommercial-NoDerivs](https://creativecommons.org/licenses/by-nc-nd/4.0/) License, which permits use and distribution in any medium, provided the original work is properly cited, the use is non-commercial and no modifications or adaptations are made.

JAHA is available at: [www.ahajournals.org/journal/jaha](http://www.ahajournals.org/journal/jaha)

## CLINICAL PERSPECTIVE

### What Is New?

- In this retrospective cohort study of patients with Loeys-Dietz syndrome, we validate cervical carotid tortuosity as a marker for risk assessment in heritable aortopathies.
- We demonstrate for the first time that total absolute curvature is a reliable biomarker, fixed during young adulthood and relatively stable over 10 years.
- Baseline total absolute curvature was predictive of aortic events during the 4-year follow-up (odds ratio [OR], 2.58 [95% CI, 1.12–5.94];  $P=0.026$ ) and remained significant after adjustment (OR, 2.64 [95% CI, 1.02–6.85];  $P=0.046$ ). Baseline tortuosity index was associated with aortic events during the 4-year follow-up (OR, 2.15 [95% CI, 1.04–4.41];  $P=0.037$ ) in univariate analysis, but not after adjustment for confounders (OR, 1.88 [95% CI, 0.79–4.51];  $P=0.157$ ).

### What Are the Clinical Implications?

- Application of this curvature-based analysis can be readily extended to centerline programs accessible to clinicians working with computed tomography/magnetic resonance imaging, offering a rapid and minimally invasive method for disease progression surveillance in patients with Loeys-Dietz syndrome.
- We specifically recommend the adoption of a curvature-based measure total absolute curvature, which is robust to confounders, as opposed to the conventional tortuosity index.
- The novelty is that the temporal association we find between total absolute curvature and outcomes related to Loeys-Dietz syndrome progression is independent of age and aging-related cardiovascular risk factors.

## Nonstandard Abbreviations and Acronyms

<b>ATI</b>	aortic tortuosity index
<b>CTA</b>	computed tomography angiogram
<b>LDS</b>	Loeys-Dietz syndrome
<b>RMS</b>	root mean square
<b>TAC</b>	total absolute curvature
<b>TI</b>	tortuosity index

Studies have demonstrated an association between vertebral or carotid arterial tortuosity and adverse aortic events in patients with heritable connective tissue disorders, including LDS, Marfan syndrome, and vascular

Ehlers-Danlos syndrome.<sup>8–10</sup> Increased tortuosity in these cases correlated with a higher likelihood of aortic dissection, rupture, and the need for surgical intervention at an earlier age.<sup>8–10</sup> However, the interpretation of these findings is limited by their use of tortuosity measurements obtained from surveillance imaging after the occurrence of associated risks like aortic dissection and early surgical intervention. Consequently, a significant gap in using arterial tortuosity as a marker of disease severity lies in the absence of a temporal relation between the measured outcomes, hindering the establishment of a clear cause-and-effect relationship.

The primary aim of this study was to investigate the association of carotid arterial tortuosity with severity of aortic phenotype in patients with LDS. Hereto, we (1) investigated the applicability and reliability of carotid arterial tortuosity as a biomarker in patients with LDS by using precise mathematical measures; (2) correlated carotid tortuosity with age, hypertension, and aortic disease status (prior aortic root surgery or type A aortic dissection) at baseline; and (3) compared carotid tortuosity among LDS subgroups based on genotypes. Secondary aims were to assess the predictive value of carotid tortuosity during follow-up on aortic root dilatation and first-time adverse aortic event (prophylactic aortic root surgery, type A aortic dissection). To measure tortuosity, we use curvature, which is an indicator of local inflection of a curve in 3-dimensional (3D) space. For curvature calculation, the fast marching method for vascular centerline computation and defining the Frenet-Serret and parallel transport frames for the resultant spatial curve are robust choices and most widely used.<sup>11–13</sup> Starting with a baseline magnetic resonance angiogram (MRA) or computed tomography angiogram (CTA) of the neck, we assessed for time-dependent increases in cervical carotid tortuosity over 10 years of follow-up. We then correlated baseline carotid tortuosity with aortic root dilatation and associated adverse outcomes in 4 years of follow-up.

We hypothesized that increased total absolute curvature, a mathematically accurate definition of tortuosity in 3D space, of the cervical carotid artery is associated with a more severe aortic phenotype and predicts aortic disease progression in patients with LDS.

## METHODS

### Study Population and Follow-Up Outcomes

This is a single-institution retrospective cohort study of patients with LDS identified from subjects enrolled in a longitudinal study from the Marfan Syndrome and Aortopathy Center at the Barnes-Jewish Hospital and Washington University School of Medicine. The

diagnosis of LDS was established based on characteristic clinical findings in the proband and family members, and identification of a pathogenic or likely pathogenic variant in *TGFBR1*, *TGFBR2*, *SMAD3*, *TGFB2*, or *TGFB3* genes. Figure 1 summarizes the study design. All patients between 14 and 75 years of age with a confirmed diagnosis of LDS by genetic testing and clinical phenotyping who were seen at the Marfan Syndrome and Aortopathy Clinic between 2010 and 2022 were assessed for eligibility (total 105 patients).<sup>14</sup> Patients were included if they had at least 1 MRA or CTA that included the total cervical carotid arteries that was available in our system. Only patients with a minimum of 2 serial CTA/MRA studies of the neck were included in the time series analysis. Angiographic exclusion criteria were poor image quality, inadequate contrast enhancement, incomplete cervical vessel imaging, or any follow-up scans taken <1 year from baseline. For patients with multiple neck angiograms, the first available CTA/MRA was designated as the baseline. Only patients with a complete, comprehensive 2-dimensional and Doppler echocardiography and a baseline neck CTA/MRA preceding the echocardiogram were included in the correlation analysis. Aortic root size was measured at the sinuses of the Valsalva using leading edge to leading edge measurements as recommended by the American Society of Echocardiography.<sup>15</sup> Echocardiographic

exclusion criteria were measurements performed after an aortic root replacement for aneurysm or type A aortic dissection. For patients with multiple echocardiograms, the latest echocardiogram was designated as the end point measurement. The study was approved by the institutional review board at the Washington University in St. Louis. The need for informed consent was waived due to the retrospective nature of the study.

Demographics, comorbidities, serial cardiovascular imaging (echocardiography and MRA/CTA studies), follow-up, and surgical data were then extracted from the electronic medical record. The primary outcomes were baseline carotid tortuosity at the time of first MRA/CTA, change in carotid tortuosity at the time of serial MRA/CTAs obtained during follow-up, maximum unoperated aortic root diameter at the time of serial echocardiograms obtained during follow-up, and the incidence of aortic event(s) (type A aortic dissection or prophylactic aortic root replacement) during follow-up. The primary end point was any first-time aortic event during 4 years of follow-up. Three measures of carotid tortuosity were computed using established mathematical formulas based on vessel path and point-wise curvature in the 3D space. Change in carotid tortuosity was expressed as a fold change from baseline ( $[(\text{final} - \text{initial}) / \text{initial}]$ ). Data are available on reasonable request from the corresponding author.

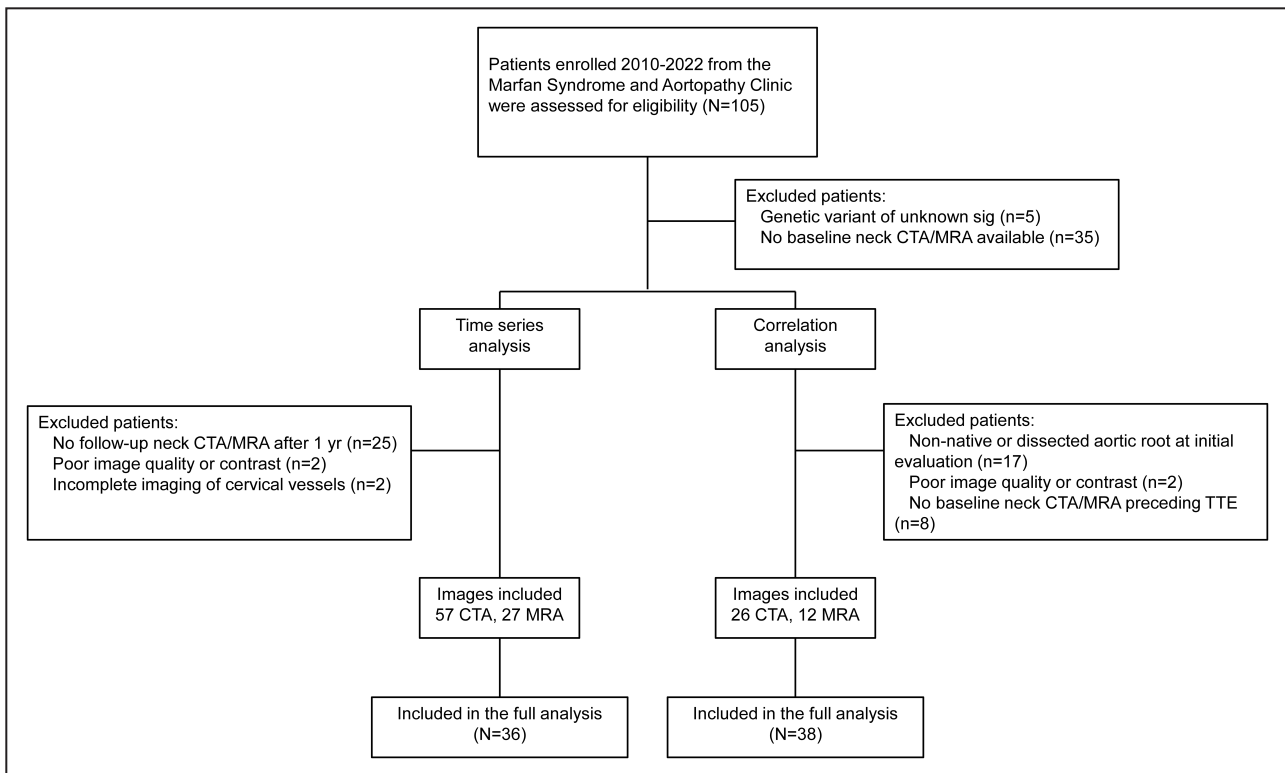


**Figure 1. Flowchart of included patients with Loey-Dietz syndrome.**

CTA, computed tomography angiography; MRA, magnetic resonance angiography; TTE, transthoracic echocardiogram; and Sig, significant.

## Image Preprocessing

Due to our inclusion of both magnetic resonance (MR)- and computed tomography (CT)-based images, data preprocessing was necessary to ensure that imaging features were calculated using the same specifications. Complete thin-layer CT images were isotropically spaced to a common voxel spacing of  $0.500 \times 0.500 \times 0.500$  mm and approximately  $0.900 \times 0.900 \times 0.900$  mm for MR images. All of the raw data were resampled using a linear interpolator to construct new data points within the range of a discrete set of known data points (ie, based on the smallest spacing from the original image). Images were then converted to vti format and processed via the Vascular Modeling Toolkit software (<http://www.vmtk.org/>) for 3D manual segmentation.

## Vessel Segmentation, 3D Reconstruction, and Geometric Analysis

Vessel segmentation, surface model generation, centerline computation, and geometric analysis follow Antiga et al.<sup>13</sup> Briefly, image segmentation was performed using implicit deformable models and the level sets method, a technique used to track the temporal evolution of the 3D embedding under image- and shape-based forces. The right and left extracranial carotid arteries were manually segmented starting with the major branches at the bifurcation off the brachiocephalic artery and the aortic arch, respectively, and terminating at the internal carotid artery petrous (C2) segment, defined by the inferior surface of the temporal bone at the external opening of the carotid canal (also referred to as the carotid foramen). After segmentation, the 0-level set surface was extracted using the marching cubes algorithm to generate a triangulated surface of the segmented vessels. Surfaces were smoothed using a nonshrinking Taubin filter and subdivided using a loop subdivision scheme to obtain a high-order representation of the surface. Centerlines were computed based on the method of solving the eikonal equation from a seed point on the Voronoi diagram domain, where each centerline point is associated with a maximal inscribed sphere that is tangent to the vessel wall at discrete locations to produce a canal surface, or tube, defined by the interpolation of maximal inscribed spheres along the centerline. Centerlines were resampled at intervals of 0.25 mm with a smoothing factor of 0.5 and 100 iterations. Point-wise curvature, torsion, maximum inscribed sphere radii, and corresponding coordinates in the xyz-space were extracted for each centerline.

## Tortuosity Measures

All measures of tortuosity are 3D and based on a geometric representation of the vessel centerline curve

(Figure 2A). Vessel length and 3 quantitative measures of tortuosity were computed for each cervical carotid artery over the length of the vessel (Figure 2B through 2D). The total length was determined by the centerline path of the 3D segmented vessel, which starts at the origin of the common carotid artery and terminates at the C2 segment of the internal carotid artery. Vessel length was estimated by summing the Euclidean distance between consecutive data points along the entire range of the curve. The formula for total length of the vessel, applied to a set of closely spaced data points ( $i, i+1, \dots, n$ ) with 3D coordinates ( $x, y, z$ ), is given by:

$$L = \sum_{i=1}^{n-1} \sqrt{(x_{i+1} - x_i)^2 + (y_{i+1} - y_i)^2 + (z_{i+1} - z_i)^2}$$

where  $L$  represents the total length of the vessel in 3D space,  $n$  is the total number of data points representing segments along the curve,  $(x_i, y_i, z_i)$  represents the coordinates of the  $i$ th data point in 3D space,  $(x_{i+1}, y_{i+1}, z_{i+1})$  represents the coordinates of the  $(i+1)$ th data point in 3D space, and  $\sum_{i=1}^{n-1}$  denotes the summation over all data points from  $i=1$  to  $n-1$ .

Tortuosity index (TI) was calculated by dividing the total length of the vessel path ( $L$ ) by the shortest distance between vessel centerline path endpoints ( $D$ ). The formula for TI, applied to a set of data points ( $i, i+1, \dots, n-1, n$ ) with 3D coordinates ( $x, y, z$ ), is given by:

$$TI = \frac{L}{D} - 1 = \frac{\sum_{i=1}^{n-1} \sqrt{(x_{i+1} - x_i)^2 + (y_{i+1} - y_i)^2 + (z_{i+1} - z_i)^2}}{\sqrt{(x_n - x_1)^2 + (y_n - y_1)^2 + (z_n - z_1)^2}} - 1$$

where  $L$ ,  $(x_i, y_i, z_i)$ , and  $\sum_{i=1}^{n-1}$  are previously defined, TI represents the tortuosity index of the vessel considering the path of the vessel in 3D space,  $D$  represents the Euclidean distance between the  $i$ th data point and the  $n$ th data point in 3D space, and  $(x_n, y_n, z_n)$  represents the coordinates of the  $n$ th data point in 3D space.

Total absolute curvature (TAC) was calculated using the Simpson rule to approximate the integral of curvature over the entire range of data points. The formula for the Simpson rule, applied to a set of equally spaced data points ( $x_i$ ) with corresponding function values ( $\kappa(x_i)$ ), is given by:

$$\int_a^b \kappa(x) dx = \frac{\Delta x}{3} \left[ \kappa(x_0) + 4 \sum_{i=1}^{n/2-1} \kappa(x_{2i}) + 2 \sum_{i=1}^{n/2} \kappa(x_{2i-1}) + \kappa(x_n) \right]$$

where  $a$  and  $b$  are the lower and upper limits of integration, respectively,  $n$  is the number of intervals between data points (or data points-1),  $x_i$  represents the  $i$ th data point,  $\kappa(x_i)$  represents the curvature value at the  $i$ th data point, and  $\Delta x$  is the spacing between data points ( $\Delta x = (b-a)/n$ ).

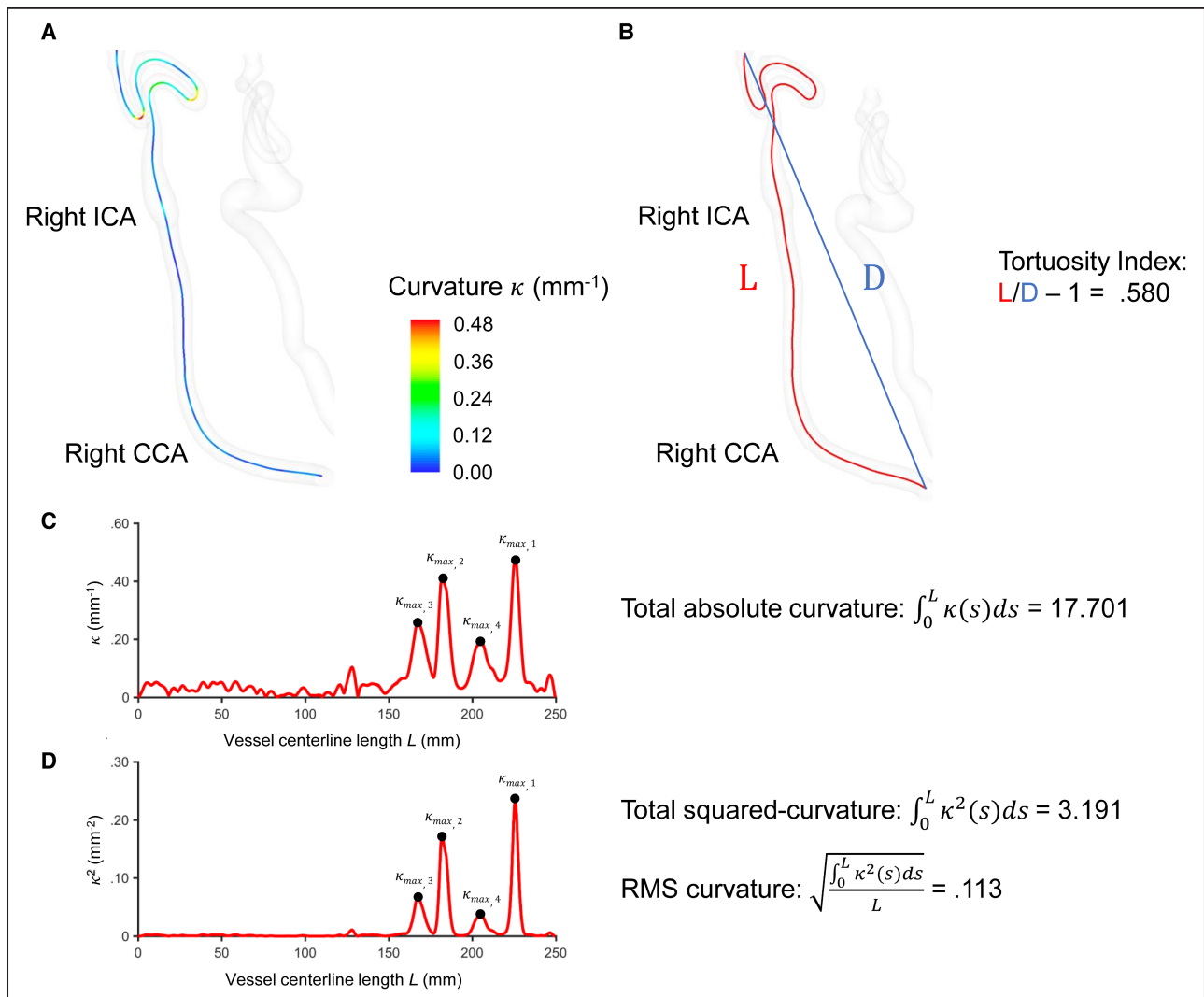


**Figure 2. Visual depiction of the tortuosity measures as derived from 3-dimensional surface models.**

The upper panel features photos of a representative cervical carotid artery using the Vascular Modeling Toolkit. **A**, Visual depiction of point-wise curvature along the vessel centerline path (or curve). Curvature at any point along the curve indicates the rate of change of curve direction over a small distance moved along the curve. Intuitively, it is a measure of how much the curve is turning. At a given point, the curvature is the inverse of the radius of the osculating circle that locally approximates the curve. The larger the curvature, the smaller the radius of the circle, the sharper the turn of the curve. **B**, The tortuosity index is the ratio of the length of the vessel centerline (L) to the Euclidean distance between its end points (D). **C**, Plot of curvature over vessel centerline path length (or arc length from origin). Total absolute curvature was calculated by approximating the integral of curvature over all closely spaced points on the curve. **D**, Plot of squared curvature over vessel centerline path length (or arc length from origin). RMS curvature was calculated by approximating the integral of squared curvature over all closely spaced points on the curve and normalized by vessel length (L).  $\kappa$ =curvature.  $S$ =a fixed point on the curve. ICA indicates internal carotid artery; CCA, common carotid artery; and RMS, root mean square.

Root mean square (RMS) curvature provides a measure of the overall smoothness or roughness curvature of a curve while considering both the magnitude and variation of curvature values. RMS curvature was calculated using the following formula:

$$\kappa_{\text{RMS}} = \sqrt{\frac{\sum_{i=1}^n \kappa^2(x_i)}{n}}$$

where  $\kappa(x_i)$  is previously defined,  $\kappa_{\text{RMS}}$  is the root mean square curvature of a curve,  $\sum_{i=1}^n$  denotes the summation over all data points from  $i=1$  to  $n$ , and  $n$  is the total

number of data points or segments along the curve. The maximum cervical carotid artery TI, TAC, and RMS curvature at the time of initial CT/MR imaging for each patient was designated the baseline carotid tortuosity.

### Statistical Analysis

Continuous variables were reported as a mean±SD or median and interquartile range (IQR). Categorical variables were reported as frequencies and percentages. Normality was assessed using the Shapiro–Wilk test. Homoscedasticity was assessed using the  $F$  test or the

nonparametric Levene test where appropriate. Linear regression analysis and the Pearson correlation coefficient ( $r$ ) were used to correlate carotid tortuosity with maximum aortic root diameter and age. The means of 2 different groups were compared with the Student  $t$  test or nonparametric Mann-Whitney  $U$  test where appropriate. Means of  $\geq 3$  groups were compared using the 1-way ANOVA test followed by post hoc Tukey honest significant difference (HSD) test for pair-wise group comparisons where appropriate. Multivariate logistic regression analysis with and without confounders was performed to identify independent predictors of the clinical end point. In the unadjusted model, carotid tortuosity (TI or TAC) is the only predictor; in the adjusted models, the presence of *TGFBR1* or *TGFBR2* mutation (yes/no), age (years), or hypertension (yes/no) are also included. Variable selection was prespecified using clinically significant variables and evaluated for significance at  $\alpha=0.10$ . Model selection was based on the probability of the log-likelihood ratio with predetermined  $\alpha=0.05$  and McFadden pseudo- $R^2 \geq 0.20$  to confirm goodness of fit. A 2-sided significance level of  $P < 0.05$  was used for each statistical test. All analyses were performed with Python version 3.11.5 in a Jupyter notebook.

## RESULTS

### Baseline Characteristics

Of the 105 patients with a diagnosis of LDS, 65 patients were included in the current study (Figure 1). Baseline characteristics are summarized in Table 1. The mean age was  $40 \pm 17$  years, and 54% were women. At the

time of baseline imaging, 17 (26%) patients had a known history of hypertension, 16 (25%) patients had undergone prophylactic aortic root replacement, and 10 (15%) patients had a prior Stanford type A aortic dissection. Mean baseline carotid tortuosity in the total cohort was  $0.262 \pm 0.131$  for TI,  $11.13 \pm 5.76$  for TAC, and  $0.212 \pm 0.188$  for RMS curvature. Patients with a history of prior aortic event(s) had a significantly higher baseline TI compared with patients with unoperated aortic roots ( $0.346 \pm 0.267$  versus  $0.195 \pm 0.164$ ;  $P=0.007$ ). Patients with a history of prior aortic event(s) had a significantly higher baseline TAC compared with patients with unoperated aortic roots ( $15.85 \pm 6.31$  versus  $10.73 \pm 5.59$ ;  $P=0.002$ ).

### Time Series Analysis

Serial cervical vessel imaging was available in 36 patients for a total of 84 angiographic images (57 CT, 27 MR) (Figure 1). Median age at the time of baseline cervical vessel imaging was 35 years (IQR, 24–42 years). Follow-up data are summarized in Table 2. A moving average filter with a 24-month time window was applied to create data grouped into discrete time points over 10 years of follow-up data (Figure 3). We performed 1-way ANOVA to compare the effect of time on change in carotid tortuosity at consecutive 24-month intervals starting from baseline (see Data S1). Mean fold change in TI at 4 to 6 years was  $0.272 \pm 0.849$  ( $P=0.696$ ) and at 8 to 10 years was  $0.302 \pm 0.656$  ( $P=0.818$ ). Mean fold change in TAC at 4 to 6 years was  $0.045 \pm 0.231$  ( $P=0.975$ ) and at 8 to 10 years was  $0.026 \pm 0.298$

**Table 1. Baseline Patient Characteristics**

Characteristic	Variable	Mean $\pm$ SD or N (%)
Demographics	Age, y	40 $\pm$ 17
	Women	35 (54%)
	Height, cm	174 $\pm$ 12
	BMI, kg/m <sup>2</sup>	25.3 $\pm$ 7.3
Pathologic mutation	<i>TGFBR1</i>	18 (28%)
	<i>TGFBR2</i>	20 (31%)
	<i>SMAD3</i>	11 (17%)
	<i>TGFB2</i>	11 (17%)
	<i>TGFB3</i>	5 (7%)
Comorbidities	Hypertension	17 (26%)
	Aortic root replacement	16 (25%)
	Type A aortic dissection	10 (15%)
	Type B aortic dissection	3 (5%)
Cervical carotid tortuosity	Vessel length, mm	206.6 $\pm$ 42.4
	Tortuosity index	0.262 $\pm$ 0.131
	Total absolute curvature	11.13 $\pm$ 5.76
	RMS curvature	0.212 $\pm$ 0.188

BMI indicates body mass index; and RMS, root mean square.

**Table 2. Serial CTA/MRA Studies and Tortuosity Outcomes During Follow-Up**

Characteristic	Variable	Median [IQR] or mean±SD	Fold change from baseline
Follow-up	Duration of follow-up, mo	54 [34–83]	...
	Total no. of serial CTA/MRA studies	2 [2–3]	...
Cervical carotid tortuosity	4–6y from baseline (n=24)		
	Tortuosity index	0.252±0.163	0.272±0.849
	Total absolute curvature	11.83±4.76	0.045±0.231
	RMS curvature	0.079±0.029	0.010±0.155
	8–10y from baseline (n=10)		
	Tortuosity index	0.164±0.118	0.302±0.656
	Total absolute curvature	10.20±4.55	0.026±0.298
	RMS curvature	0.074±0.034	−0.030±0.336

CTA indicates computed tomography angiography; IQR, interquartile range; MRA: magnetic resonance angiography; and RMS, root mean square.

( $P=1.000$ ). There were no significant differences between the means of change in TI, TAC, or RMS curvature for any pair of different 24-month intervals of time over 10 years of follow-up (Tables S1 through S3, respectively). These data validate the use of patient-specific carotid tortuosity values designated as baseline in the correlation analysis. Moreover, the tight error bars for changes in TAC and changes in RMS curvature at each time point (depicted in Figure 3B and 3C, respectively), in contrast to the wide variance in changes in TI (depicted in Figure 3A), suggest the more appropriate use of curvature-based measures of tortuosity as a reliable quantitative marker.

### Correlation Analysis

Unoperated aortic root diameters were available in 38 patients (Figure 1), of whom 13 subsequently experienced an aortic event (11 prophylactic aortic root replacement, 3 type A aortic dissection). Median follow-up time from baseline to latest echocardiogram was 36 months (IQR, 11–64 months). Median maximum aortic root diameter was 3.9 cm (IQR, 3.5–4.3 cm). Baseline TAC was significantly associated with maximum unoperated aortic root diameter ( $r=0.456$ ,  $P=0.004$ ); baseline TI was significantly associated with maximum unoperated aortic root diameter ( $r=0.342$ ,  $P=0.036$ ), although to a lesser degree. To account for confounding factors, the relationship between carotid tortuosity and age was also analyzed. Baseline TAC was significantly associated with age ( $r=0.370$ ,  $P=0.019$ ); baseline TI was significantly associated with age ( $r=0.532$ ,  $P<0.001$ ) with a greater degree of correlation. Detailed linear regression and correlation analyses are provided in Figure 4. Patients who developed an aortic event during follow-up had a significantly higher baseline TAC compared with nonevent patients ( $11.01±5.63$  versus  $8.63±4.86$ ;  $P=0.049$ ). The difference in baseline TI between patients who developed an aortic event

and nonevent patients was not statistically significant ( $0.192±0.146$  versus  $0.142±0.137$ ;  $P=0.132$ ).

We performed logistic regression analyses for baseline carotid tortuosity (TI or TAC) with and without adjustment for potential confounders and the binary end point of aortic event within 4 years during follow-up. This analysis included patients with at least 1 neck CTA/MRA, considered to be the baseline, with a minimum 4 years of follow-up. We analyzed the end point of any aortic event (type A aortic dissection or prophylactic aortic root replacement) during 4 years of follow-up. Patients with a nonnative or dissected aortic root at the time of baseline angiogram were excluded from the data, and only data obtained at the time of baseline angiogram were used as variables. The predictor of main interest in this analysis is our curvature-based measure of carotid tortuosity (TAC), and the model was adjusted for the presence of hypertension (yes/no), age (years), and the presence of a *TGFBR1* or *TGFBR2* mutation (yes/no).

Of the 40 patients analyzed for clinical end point, 11 patients (28%) developed an aortic event during 4 years of follow-up and a total of 15 patients (38%) during the entire follow-up. The odds ratio (OR) of an aortic event occurring within 4 years for a 1-SD increment in baseline TAC was 2.58 (95% CI, 1.12–5.94;  $P=0.026$ ) in univariate analysis and after adjustment was 2.64 (95% CI, 1.02–6.85;  $P=0.046$ ). The discrepancy between adjusted and unadjusted estimates is <3%, indicating that there is little confounding of the effect of TAC as a result of the other covariates in the adjusted model. The effects of age, hypertension, and *TGFBR1/2* are not larger than could be due to chance in these data ( $P>0.05$ ). The OR of an aortic event occurring within 4 years for a 1-SD increment in baseline TI was 2.15 (95% CI, 1.04–4.41;  $P=0.037$ ) in univariate analysis and after adjustment was 1.88 (95% CI, 0.79–4.51;  $P=0.157$ ). Age, hypertension, and *TGFBR1/2* mutation were nonsignificant predictors but had a confounding

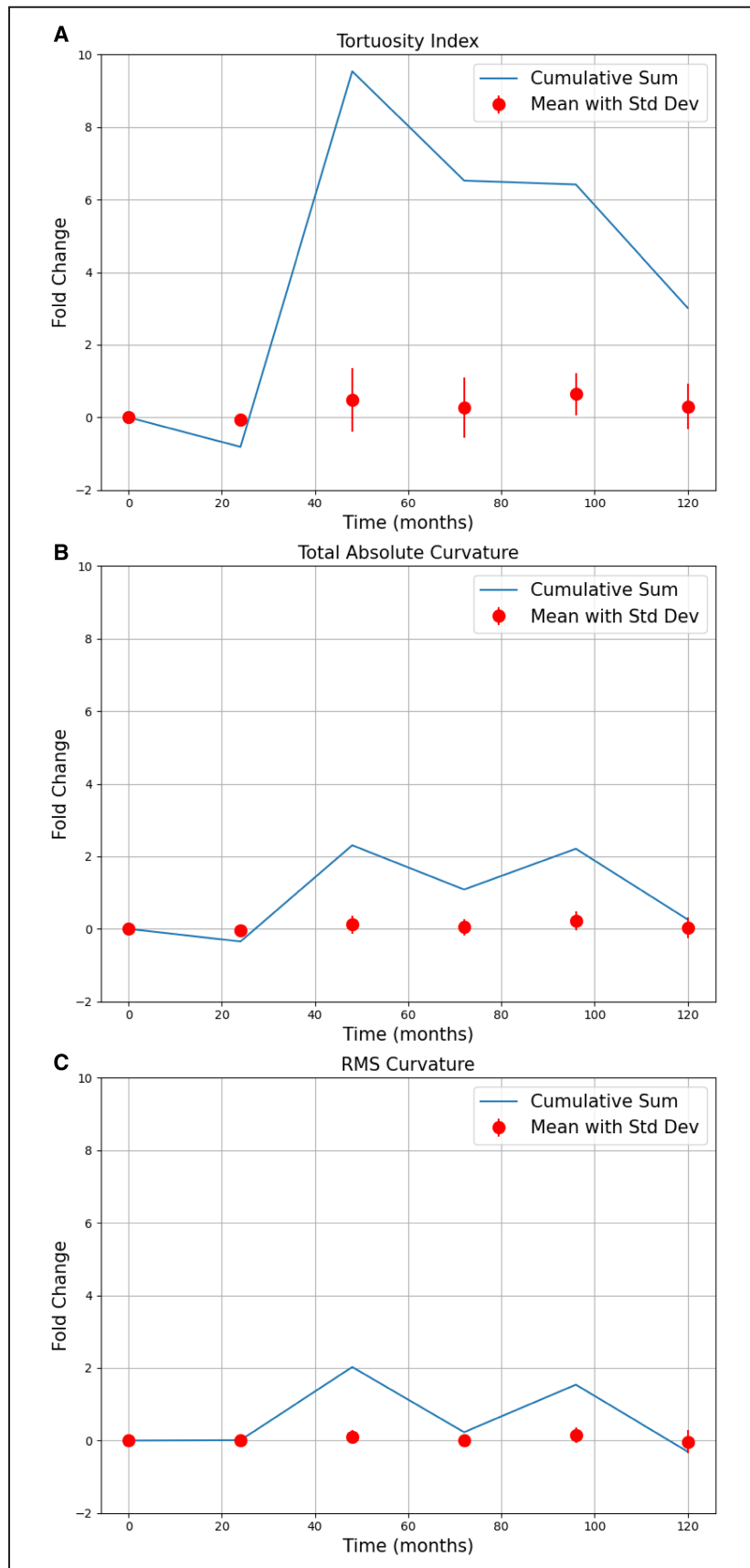




**Figure 3. Change in tortuosity from baseline over 10 years of follow-up.**

Primary data were processed with a 24-month moving average filter. The data points represent the mean for each 24-month window of the x axis, and error bars represent the standard deviation. The blue line tracks a cumulative sum throughout the different 24-month windows of the x axis, from baseline to 120 months. Data points represent the following number of patients: 0 to 24 months, N=12; 24 to 48 months, N=10; 48 to 72 months, N=24; 72 to 96 months, N=10; 96 to 120 months, N=10. **A**, Tortuosity index. **B**, Total absolute curvature. **C**, RMS curvature. RMS indicates root mean square; and SD, standard deviation.

effect on TI in the adjusted model. Detailed univariable and multivariable ORs are listed in [Table 3](#).

On receiver operating curve analysis, both the baseline TI (area under the curve=0.737;  $P=0.029$ ) and the baseline TAC (area under the curve=0.724;  $P=0.014$ ) were good discriminators of patients who developed an aortic event during 4 years of follow-up ([Figure 5A](#) and [5B](#), respectively). However, TAC was the only independent predictor of aortic events identified in multivariate analyses and also demonstrated robustness against confounders. Altogether, these results suggest that the effects of TI are likely due to its correlation with TAC, based on the mathematical definition of tortuosity in 3D space, rather than being a direct measure of arterial tortuosity.

## DISCUSSION

The objective of our work was 2-fold: (1) to investigate the temporal relationship between cervical carotid tortuosity and outcomes related to disease progression and (2) to validate a curvature-based marker of cervical carotid tortuosity for risk stratification in patients with LDS.

The current study provides evidence of a meaningful temporal link between carotid tortuosity and aggressive aortic disease in inherited aortopathies. We found that baseline carotid tortuosity was predictive of subsequent aortic root dilatation and associated adverse outcomes (type A aortic dissection or prophylactic aortic root replacement) during 4 years of follow-up. We also demonstrated that carotid tortuosity, on average, is relatively stable over 10 years of follow-up in a cohort of pediatric and adult patients with LDS. Our curvature-based measure, TAC in particular, correlates strongly with aortic outcomes and was robust to confounders including age, hypertension, and *TGFBR1/2* mutation. Altogether, our results suggest that increased cervical carotid artery tortuosity, which appears to be fixed in quantity, may be a marker of advanced disease progression in LDS.

A critical barrier to using arterial tortuosity as a marker for severe disease in LDS and other heritable aortopathies is the lack of a clear causal or direct correlative relationship. Specifically, there are 2 limitations due to confounding factors: age and time. Prior studies assessing arterial tortuosity as a marker for adverse outcomes have circumvented the first potential confounding factor by limiting their data to ages

<50 years,<sup>8,10</sup> based on evidence that arterial tortuosity has less discrimination in older subjects due to the natural development of tortuosity with aging. Morris et al found an association between increased vertebral tortuosity index and the end point of cardiac surgery before 10 years of age in patients with heritable connective tissue disorders,<sup>8</sup> mostly Marfan syndrome and LDS. Stephens et al developed a height-adjusted vertebral tortuosity index and found an association between height-adjusted vertebral tortuosity index and the occurrence of a cardiovascular event before 30 years of age (area under the curve=0.71).<sup>10</sup> In multivariate analysis, they found that older age was the only factor associated with increased cardiovascular event rate, whereas height-adjusted vertebral tortuosity index was not; however, height-adjusted vertebral tortuosity index was associated with events among those with high-risk variants <40 years of age, suggesting effect modification by genotype and age.<sup>10</sup> It also suggests that the effect of height is only significant in patients <40 years of age. These inconsistent findings may, in part, be related to the use of TI as a measure of arterial tortuosity.

The lack of an accurate and standardized assessment of tortuosity may be another barrier to the use of arterial tortuosity as a marker. We demonstrate that TI, a widely used but less accurate measure of arterial tortuosity, does not consistently correlate with aortic outcomes when controlling for time elapsed between measurement and clinical end point (ie, using a baseline measure of carotid tortuosity taken 4 years before outcomes analysis). For example, patients with a history of prior aortic dissection or surgery at baseline had a significantly greater TI compared with nonevent patients ( $0.346\pm 0.267$  versus  $0.195\pm 0.164$ ;  $P=0.007$ ). However, when comparing mean baseline TI in patients with unoperated aortic roots, there was no significant difference between patients who developed an aortic event within 4 years compared with nonevent patients ( $0.192\pm 0.146$  versus  $0.142\pm 0.137$ ;  $P=0.132$ ). By comparison, mean baseline TAC was significantly higher in patients with a prior aortic event compared with nonevent patients ( $15.85\pm 6.31$  versus  $10.73\pm 5.59$ ;  $P=0.002$ ) and also in patients who developed an aortic event within 4 years compared with nonevent patients ( $11.01\pm 5.63$  versus  $8.63\pm 4.86$ ;  $P=0.049$ ). Moreover, the association of TI with the occurrence of aortic events was not significant after adjustment for clinically significant confounders.

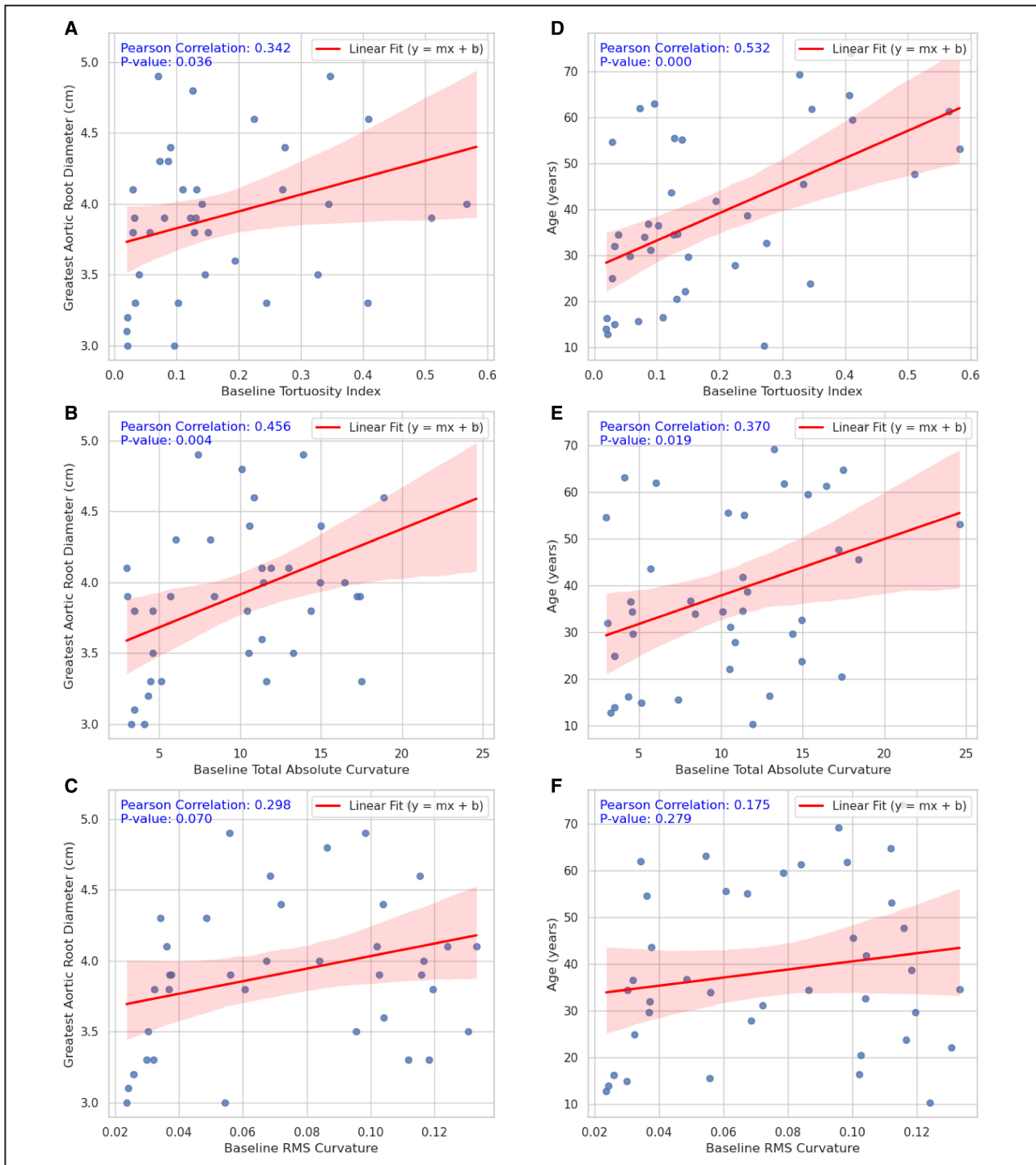


**Figure 4. Baseline tortuosity in relation to maximum unoperated aortic root diameter (A through C) and age (D through F).** Data represent N=40 patients in each plot. **A**, Maximum unoperated aortic root diameter vs tortuosity index. **B**, Maximum unoperated aortic root diameter vs total absolute curvature. **C**, Maximum unoperated aortic root diameter vs RMS curvature. **D**, Age vs tortuosity index. **E**, Age vs total absolute curvature. **F**, Age vs RMS curvature. RMS indicates root mean square.

Tortuosity of the carotid artery, a medium-sized elastic artery, may reflect an underlying arteriopathy and 1 manifestation of a generalized disease process in heritable connective tissue disorders. In a retrospective study of patients with Marfan syndrome, Franken

et al reported similar findings using tortuosity of the aorta, a large-sized elastic artery, and found strong associations between baseline aortic tortuosity index (ATI) and aortic dilatation rate and the occurrence of aortic events (type B aortic dissection or aortic

**Table 3. Tortuosity Variables and Odds Ratios for Adverse Aortic Events 4 Years From Baseline**

Logistic regression model	Unadjusted				Adjusted			
	Predictor	OR	95% CI	P value	Predictor	OR	95% CI	P value
1	Tortuosity index (1 SD)	2.15	1.04–4.41	0.037	Tortuosity index (1 SD)	1.88	0.79–4.51	0.157
					<i>TGFBR1</i> or <i>TGFBR2</i>	1.59	0.70–3.63	0.270
					Age (1 y)	1.25	0.51–3.07	0.624
					Hypertension	1.04	0.49–2.20	0.917
2	Total absolute curvature (1 SD)	2.58	1.12–5.94	0.026	Total absolute curvature (1 SD)	2.64	1.02–6.85	0.046
					<i>TGFBR1/TGFBR2</i>	1.91	0.77–4.73	0.163
					Age (1 y)	1.22	0.51–2.99	0.648
					Hypertension	1.03	0.49–2.17	0.934

1 SD for tortuosity index=0.157; 1 SD for total absolute curvature=5.33. OR indicates odds ratio.

surgery) during 3 years of follow-up.<sup>16</sup> Multivariate analysis identified ATI and aortic root diameter as the only independent predictors for aortic events, whereas ATI had the largest discriminating power for aortic dissection alone.<sup>16</sup> The effects of ATI were found to be independent of sex, age, body surface area, aortic volume, and losartan use,<sup>16</sup> suggesting that ATI was also robust against clinically significant confounders and potentially a stable marker in Marfan syndrome.

Cervical carotid tortuosity, using a curvature-based measure, may be a biomarker for more severe disease phenotype in LDS, irrespective of age and pending disease progression for years in advance. Although cervical carotid tortuosity is known to increase with older age and is classically associated with hypertension-induced vascular structural changes,<sup>17</sup> it did not change significantly over 10 years of follow-up in our patients with LDS. Carotid tortuosity may also serve as an indicator of disease severity for years following the occurrence of an adverse event, evidenced

by our finding of increased carotid TAC in patients with a history of aortic events at baseline compared with the patients with an unoperated aortic root (15.85±6.31 versus 10.73±5.59; *P*=0.002). Although the current study is neither designed nor powered a priori for risk stratification, we observed a trend toward stratified levels of carotid tortuosity based on the onset of first aortic event, the highest TAC in patients with a prior history of aortic event (15.85±6.31), followed by patients who had their first aortic event in the subsequent 4 years (11.01±5.63), and then lowest TAC in patients who remained event-free during the study period (8.63±4.86).

We acknowledge that our study has limitations. First, the small sample size limits the number of variables that can be included in regression analyses. With our *N*=40 patients eligible for logistic regression, we are limited to 2 to 4 variables. Strategic selection of covariates based on prior knowledge and published data on arterial tortuosity, especially for medium-sized arteries in heritable connective tissue

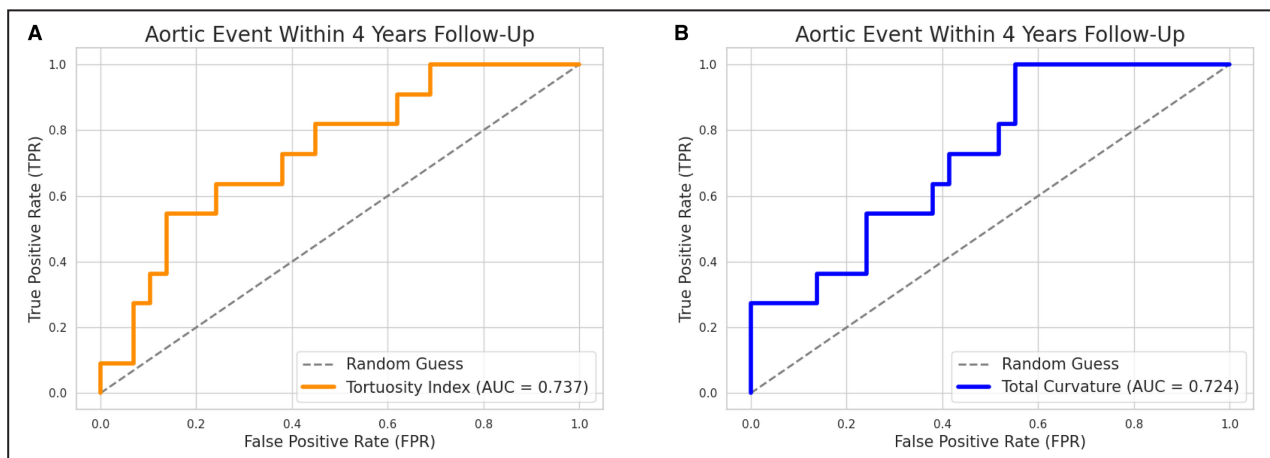


**Figure 5. Receiver operating curves using baseline carotid tortuosity to predict the occurrence of adverse aortic event within 4 years.**

Data represent *N*=40 patients in each plot. **A.** Tortuosity index. **B.** Total absolute curvature. AUC indicates area under the curve; FPR, false positive rate; and TPR, true positive rate.

disorders, helped to discriminate potential confounding factors in our analysis. Second, the use of survival analysis methods to account for varying length of follow-up may be an appropriate assessment of the time-to-event data. Future studies may benefit from developing models that account for the presence of disease-causing variants in the *TGFBR1* or *TGFBR2* gene, which are known to manifest clinically as more aggressive aortic diseases with increased arterial tortuosity,<sup>18,19</sup> and perhaps also in *TGFB3*, which is reported to have less aggressive arteriopathy than other LDS variants,<sup>20,21</sup> to better elucidate the effect of LDS genetic variant on severity of aortic phenotype (or as a confounder in the effect of carotid tortuosity). Finally, pooling data from longitudinal studies to compare the relationships between carotid tortuosity and the severity of aortopathies for various inherited connective disorders may help to identify robust markers for risk stratification.

## CONCLUSIONS

Here we introduce cervical carotid tortuosity as a promising quantitative biomarker with validated, standardized characteristics. Increased carotid tortuosity is associated with a more severe aortic phenotype in patients with LDS and predicts aortic disease progression during follow-up. Specifically, we recommend the adoption of a curvature-based measure TAC, which is reliable (less inherent variability) and precise (less prone to measurement errors), for early detection or monitoring of disease progression in LDS. TI, by definition, varies greatly depending on the selection of end points and is difficult to standardize between vascular anatomy where the bifurcation or origin and terminus are not fixed. The application of this curvature-based analysis can be readily extended to centerline programs accessible to clinicians working with CT/MR imaging. Calculating the 3D point-wise curvature from a set of centerline points (using the Frenet-Serret formulas) involves few steps. First, obtain centerline points representing the path of interest. This can be achieved by extracting centerline points from medical imaging data (MR imaging or CT scans) via workspace software. For each point on the centerline, calculate the tangent vector, the normal vector, and the binormal vector. These steps can be implemented in Python using libraries like NumPy for vector operations and SciPy for interpolation to help you efficiently compute the curvature from centerline points. Once you have the tangent, normal, and binormal vectors for each point, curvature can be calculated using the Frenet-Serret formulas, and TAC can be calculated using our curvature-based analysis.

## ARTICLE INFORMATION

Received February 27, 2024; accepted May 16, 2024.

### Affiliations

Department of Neurological Surgery, Washington University School of Medicine, St. Louis, MO (J.V.L., A.L.H., R.G.D., J.W.O.); Department of Biomedical Engineering, Washington University in St. Louis, St. Louis, MO (J.V.L.); and Cardiovascular Division, Department of Medicine, Washington University School of Medicine, St. Louis, MO (A.C.B.).

### Acknowledgments

Author contributions: Study concept and design: J.V. Lee and Drs Huguenard, Braverman, Dacey, Osbun. Acquisition of data: J.V. Lee and Dr Huguenard. Formal analysis and software: J.V. Lee. Interpretation of data: J.V. Lee and Drs Huguenard, Dacey, and Braverman. Drafting of the article: J.V. Lee. All authors critically reviewed, edited, and approved the final version of the article. Statistical analysis: J.V. Lee. Study supervision: Drs Huguenard, Dacey, Braverman, and Osbun.

### Sources of Funding

None.

### Disclosures

None.

### Supplemental Material

Data S1  
Tables S1–S3

## REFERENCES

1. Welby JP, Kim ST, Carr CM, Lehman VT, Rydberg CH, Wald JT, Luetmer PH, Nasr DM, Brinjikji W. Carotid artery tortuosity is associated with connective tissue diseases. *Am J Neuroradiol*. 2019;40:1738–1743. doi: [10.3174/ajnr.A6218](https://doi.org/10.3174/ajnr.A6218)
2. Isselbacher EM, Preventza O, Hamilton Black J III, Augoustides JG, Beck AW, Bolen MA, Braverman AC, Bray BE, Brown-Zimmerman MM, Chen EP, et al. 2022 ACC/AHA guideline for the diagnosis and management of aortic disease: a report of the American Heart Association/American College of Cardiology Joint Committee on clinical practice guidelines. *Circulation*. 2022;146:e334–e482. doi: [10.1161/CIR.0000000000001106](https://doi.org/10.1161/CIR.0000000000001106)
3. Loeys BL, Schwarze U, Holm T, Callewaert BL, Thomas GH, Pannu H, De Backer JF, Oswald GL, Symoens S, Manouvrier S, et al. Aneurysm syndromes caused by mutations in the TGF- $\beta$  receptor. *N Engl J Med*. 2006;355:788–798. doi: [10.1056/NEJMoa055695](https://doi.org/10.1056/NEJMoa055695)
4. Coulon C. Thoracic aortic aneurysms and pregnancy. *Presse Med*. 2015;44:1126–1135. doi: [10.1016/j.jpm.2015.02.024](https://doi.org/10.1016/j.jpm.2015.02.024)
5. Jondeau G, Boileau C. Genetics of thoracic aortic aneurysms. *Curr Atheroscler Rep*. 2012;14:219–226. doi: [10.1007/s11883-012-0241-4](https://doi.org/10.1007/s11883-012-0241-4)
6. Baumgartner H, Falk V, Bax JJ, De Bonis M, Hamm C, Holm PJ, Jung B, Lancellotti P, Lansac E, Rodriguez Muñoz D, et al. ESC scientific document group. 2017 ESC/EACTS guidelines for the management of valvular heart disease. *Eur Heart J*. 2017;38:2739–2791. doi: [10.1093/eurheartj/ehx391](https://doi.org/10.1093/eurheartj/ehx391)
7. Krohg-Sørensen K, Lingaas PS, Lundblad R, Seem E, Paus B, Geiran OR. Cardiovascular surgery in Loeys–Dietz syndrome types 1–4. *Eur J Cardiothorac Surg*. 2017;52:1125–1131. doi: [10.1093/ejcts/ezx147](https://doi.org/10.1093/ejcts/ezx147)
8. Morris SA, Orbach DB, Geva T, Singh MN, Gauvreau K, Lacro RV. Increased vertebral artery tortuosity index is associated with adverse outcomes in children and young adults with connective tissue disorders. *Circulation*. 2011;124:388–396. doi: [10.1161/CIRCULATIONAHA.110.990549](https://doi.org/10.1161/CIRCULATIONAHA.110.990549)
9. Chu LC, Haroun RR, Beaulieu RJ, Black JH, Dietz HC, Fishman EK. Carotid artery tortuosity index is associated with the need for early aortic root replacement in patients with Loeys-Dietz syndrome. *J Comput Assist Tomogr*. 2018;42:747–753. doi: [10.1097/RCT.0000000000000764](https://doi.org/10.1097/RCT.0000000000000764)
10. Stephens SB, Shalhub S, Dodd N, Li J, Huang M, Oda S, Kancherla K, Doan TT, Prakash SK, Weigand JD, et al. Vertebral tortuosity is associated with increased rate of cardiovascular events in vascular Ehlers-Danlos syndrome. *J Am Heart Assoc*. 2023;12:e029518. doi: [10.1161/JAHA.123.029518](https://doi.org/10.1161/JAHA.123.029518)

11. Piccinelli M, Veneziani A, Steinman DA, Remuzzi A, Antiga L. A framework for geometric analysis of vascular structures: application to cerebral aneurysms. *IEEE Trans Med Imaging*. 2009;28:1141–1155. doi: [10.1109/TMI.2009.2021652](https://doi.org/10.1109/TMI.2009.2021652)
12. Antiga L, Steinman DA. Robust and objective decomposition and mapping of bifurcating vessels. *IEEE Trans Med Imaging*. 2004;23:704–713. doi: [10.1109/TMI.2004.826946](https://doi.org/10.1109/TMI.2004.826946)
13. Antiga L, Piccinelli M, Botti L, Ene-Iordache B, Remuzzi A, Steinman DA. An image-based modeling framework for patient-specific computational hemodynamics. *Med Biol Eng Comput*. 2008;46:1097–1112. doi: [10.1007/s11517-008-0420-1](https://doi.org/10.1007/s11517-008-0420-1)
14. Huguenard AL, Johnson GW, Osbun JW, Dacey RG, Braverman AC. Frequency of screening-detected intracranial aneurysms in patients with Loeys-Dietz syndrome. *Circulation*. 2022;146:142–143. doi: [10.1161/CIRCULATIONAHA.122.058948](https://doi.org/10.1161/CIRCULATIONAHA.122.058948)
15. Lang RM, Badano LP, Mor-Avi V, Afilalo J, Armstrong A, Ernande L, Flachskampf FA, Foster E, Goldstein SA, Kuznetsova T, et al. Recommendations for cardiac chamber quantification by echocardiography in adults: an update from the American Society of Echocardiography and the European Association of Cardiovascular Imaging. *J Am Soc Echocardiogr*. 2015;28:1–39.e14. doi: [10.1016/j.echo.2014.10.003](https://doi.org/10.1016/j.echo.2014.10.003)
16. Franken R, El Morabit A, de Waard V, Timmermans J, Scholte AJ, van den Berg MP, Marquering H, Planken NRN, Zwinderman AH, Mulder BJM, et al. Increased aortic tortuosity indicates a more severe aortic phenotype in adults with Marfan syndrome. *Int J Cardiol*. 2015;194:7–12. doi: [10.1016/j.ijcard.2015.05.072](https://doi.org/10.1016/j.ijcard.2015.05.072)
17. Ciurică S, Lopez-Sublet M, Loeys BL, Radhouani I, Natarajan N, Vikkula M, Maas AHEM, Adlam D, Persu A. Arterial tortuosity. *Hypertension*. 2019;73:951–960. doi: [10.1161/HYPERTENSIONAHA.118.11647](https://doi.org/10.1161/HYPERTENSIONAHA.118.11647)
18. Rodrigues VJ, Elsayed S, Loeys BL, Dietz HC, Yousem DM. Neuroradiologic manifestations of Loeys-Dietz syndrome type 1. *AJNR Am J Neuroradiol*. 2009;30:1614–1619. doi: [10.3174/ajnr.A1651](https://doi.org/10.3174/ajnr.A1651)
19. Jondeau G, Ropers J, Regalado E, Braverman A, Evangelista A, Teixedo G, De Backer J, Muñoz-Mosquera L, Naudion S, Zordan C, et al. Montalcino aortic consortium. International registry of patients carrying TGFBR1 or TGFBR2 mutations: results of the MAC (Montalcino aortic consortium). *Circ Cardiovasc Genet*. 2016;9:548–558. doi: [10.1161/CIRCGENETICS.116.001485](https://doi.org/10.1161/CIRCGENETICS.116.001485)
20. Braverman AC. Heritable thoracic aortic aneurysm disease: recognizing phenotypes, exploring genotypes. *J Am Coll Cardiol*. 2015;65:1337–1339. doi: [10.1016/j.jacc.2014.12.056](https://doi.org/10.1016/j.jacc.2014.12.056)
21. Bertoli-Avella AM, Gillis E, Morisaki H, Verhagen JMA, de Graaf BM, van de Beek G, Gallo E, Kruihof BPT, Venselaar H, Myers LA, et al. Mutations in a TGF- $\beta$  ligand, TGFB3, cause syndromic aortic aneurysms and dissections. *J Am Coll Cardiol*. 2015;65:1324–1336. doi: [10.1016/j.jacc.2015.01.040](https://doi.org/10.1016/j.jacc.2015.01.040)